

RSC Advances



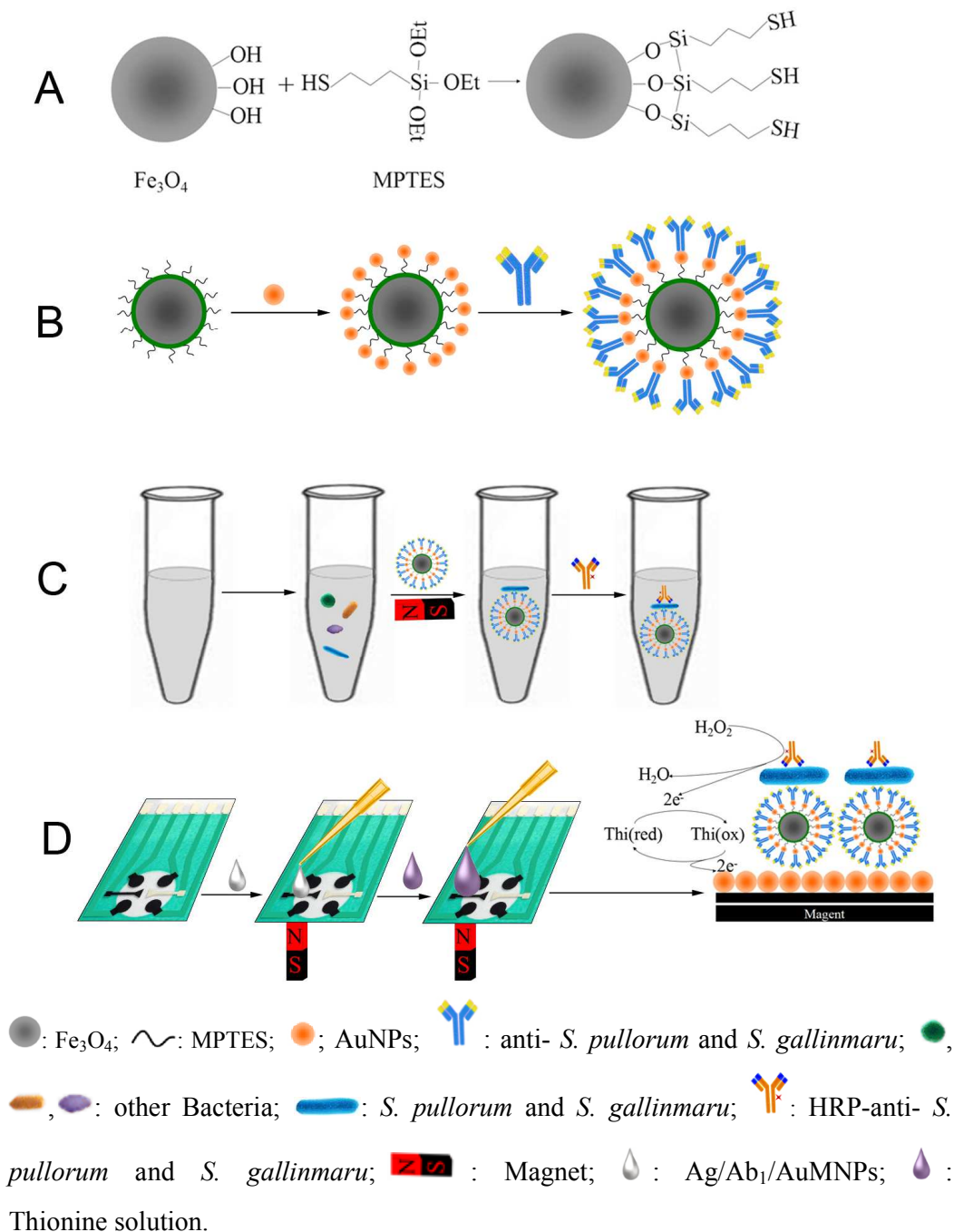
This is an *Accepted Manuscript*, which has been through the Royal Society of Chemistry peer review process and has been accepted for publication.

Accepted Manuscripts are published online shortly after acceptance, before technical editing, formatting and proof reading. Using this free service, authors can make their results available to the community, in citable form, before we publish the edited article. This *Accepted Manuscript* will be replaced by the edited, formatted and paginated article as soon as this is available.

You can find more information about *Accepted Manuscripts* in the [Information for Authors](#).

Please note that technical editing may introduce minor changes to the text and/or graphics, which may alter content. The journal's standard [Terms & Conditions](#) and the [Ethical guidelines](#) still apply. In no event shall the Royal Society of Chemistry be held responsible for any errors or omissions in this *Accepted Manuscript* or any consequences arising from the use of any information it contains.

Graphical Abstract: The preparation of immunoassay method has been showed in Schematic illustrations: (A) The synthesis of $\text{Fe}_3\text{O}_4/\text{SiO}_2\text{-SH}$; (B) AuNPs and Ab_1 link with $\text{Fe}_3\text{O}_4/\text{SiO}_2\text{-SH}$ based on the self-assembly in order; (C) Functions of IMB for antigen (Ag) enrichment and separation from sample, and HRP-antibody (HRP- Ab_2) for immunoreaction; (D) HRP- $\text{Ab}_2/\text{Ag}/\text{Ab}_1/\text{AuMNP}$ s dropped on the AuNPs/4-SPCE, the principle of electrochemical detection.



1 **A sandwich electrochemical immunoassay for *Salmonella***
2 ***pullorum* and *Salmonella gallinarum* based on**
3 **AuNPs/SiO₂/Fe₃O₄ adsorpting antibody and 4 channels screen**
4 **printed carbon electrode electrodeposited gold nanoparticles**

5 Jianfeng Fei, Wenchao Dou*, Guangying Zhao¹

6 *Food Safety Key Lab of Zhejiang Province, College of Food Science and*
7 *Biotechnology Engineering, Zhejiang Gongshang University, Hangzhou 310018, PR*
8 *China*

9

¹ *Corresponding author.

E-mail address: zhaogy-user@163.com (G. Zhao); wdou@zjsu.edu.cn (W. Dou).

10

11 **ABSTRACT** A rapid and high-sensitive sandwich electrochemical immunoassay method
12 was constructed for *Salmonella pullorum* and *Salmonella gallinarum* (*S. pullorum* and *S.*
13 *gallinarum*) determination based on immune magnetic beads (MB) and enzyme labeled
14 antibody. An abundance of gold nanoparticles (AuNPs) were attached to SiO₂ coated
15 Fe₃O₄ nanoparticles (Fe₃O₄/SiO₂) via the covalent binding between the -SH groups of the
16 Fe₃O₄/SiO₂ and AuNPs. Antibodies against *S. pullorum* and *S. gallinarum* were
17 immobilized on Fe₃O₄/SiO₂/AuNPs nanocomposites (AuMNPs) by automatic adsorption
18 between thiol and AuNPs. *S. pullorum* and *S. gallinarum* in sample were captured by
19 AuMNPs and separated from samples by applying an external magnetic field. The
20 AuMNPs–*Salmonella* complexes (Ag/Ab₁/AuMNPs) were re-dispersed a buffer solution
21 then exposed to Horseradish Peroxidase-labeled anti- *S. pullorum* and *S. gallinarum*
22 (HRP-Ab₂) solution, forming a sandwich-type immune complex
23 (HRP-Ab₂/Ag/Ab₁/AuMNPs). 4 channels screen printed carbon electrode (4-SPCE) was
24 modified by gold nanoparticles (AuNPs) through electrodeposition method to prepare
25 AuNPs/4-SPCE. After magnetically separating the sandwich immune complexes from
26 solution, the HRP-Ab₂/Ag/Ab₁/AuMNPs was anchored on AuNPs/4-SPCE by magnet. A
27 linear response to *S. pullorum* and *S. gallinarum* was obtained in concentration range
28 from 10² to 10⁶ CFU·mL⁻¹, with a limit of detection of 3.2×10¹ CFU·mL⁻¹ (at an SNR of
29 3). This nanoparticle-based immunoassay method offers a way of sensitive, highly
30 specific, and reproducible detection of *S. pullorum* and *S. gallinarum*. Given its low
31 detection limit, it represents a promising potential in detection for other food-borne
32 pathogens by exchanging the antibody.

33 **Keywords:** Electrochemical sensor; Gold nanoparticles; Fe₃O₄/SiO₂/AuNPs; Sandwich
34 assay; *Salmonella*.

35

36

37

38 1. Introduction

39 Research on electrochemical immunoassay has attracted more attention from
40 scientists in recent years. Such research can be easily conducted using simple
41 electrochemical instruments that have the potential of miniaturization and automation ^{1,2}.
42 Electrochemical immunoassays that capitalize on the selectivity of antigen-antibody
43 reactions have excellent detection limits and selectivity. Moreover, it is not affected by
44 the sample components that might interfere with spectroscopic detection, such as
45 particles, chromophores, and fluorophores ³. Thus, the electrochemical immunosensor is
46 very suitable to detect food-borne pathogens in complex sample without interference
47 from matrix with excellent selectivity, reproducibility and usability ^{4,5}.

48 Antibody immobilization is vital in successful development of an electrochemical
49 immunosensor, and the present immobilization methods, such as chemical modification,
50 self-assembly, or physical absorption, are usually quite complex and liable to make the
51 antibody deactivate in real application ⁶⁻⁸. So if the antibody modification procedure can
52 be excluded, there will be a good prospect for the method. The Horseradish Peroxidase
53 (HRP) can biocatalyze H₂O₂ in the presence of thionine, resulting in an obviously
54 increase of the redox and reduction peak of Cyclic Voltammetry (CV) ⁹. The above
55 detection principle has been widely used in the development of novel electrochemical
56 immunosensor. If enriching the amount of above sandwich complexes accumulated on
57 working electrode, the sensitivity of the immunoassay would be greatly improved ¹⁰.

58 More recently, magnetic nanoparticles (MNPs) have received increasing attention
59 due to their high surface-to-volume ratios, allowing for the direct capture, easy separation
60 and concentration of targets in complex samples in an external magnetic field. MNPs are
61 superparamagnetic, which means that they are attracted to a magnetic field but retain no
62 residual magnetism after the field is removed ¹¹. Therefore, MNPs tagged to the
63 biomaterial of interest can be removed from a matrix using a magnetic field, but they do
64 not agglomerate after removal of the field. These advantages make MNPs desirable
65 candidates for electrochemical immunoassay, as they can function as both an amplifier to
66 increase the sensitivity of the electrochemical immunoassay and simultaneously as a
67 concentration purification agent to reduce background interference ^{12,13}. Although MNPs
68 are excellent agents for a low-interference and sensitive electrochemical immunoassay,

69 they suffer from several drawbacks such as a lack of surface tunability for biocompatible
70 applications, which makes them difficult to couple with biomolecules directly¹⁴. However,
71 if the proteins were immobilized directly on the surface of MNPs, pure magnetic particles
72 may undergo rapid biodegradation when they are directly exposed to complex
73 environmental and biological systems¹⁰. Therefore, a suitable coating is essential to
74 prevent such limitations from occurring. Silica has been reported to be one of the best
75 candidate shell materials for the fabrication of novel magnetic core-shell MNPs/ SiO₂,
76 exhibiting the desirable intrinsic properties of the magnetic core and silica shell¹⁵.

77 It is well known that gold nanoparticles (AuNPs) possess the property of high
78 stability and good biocompatibility¹⁶. The surface of gold nanoparticles (AuNPs) can be
79 coated with antibody based on the automatic adsorption between antibody and AuNPs,
80 and AuNPs can retain high bioactivity of the adsorbed biomolecules^{17, 18}. Thus,
81 combining MNPs with silicon dioxide and AuNPs shell (Fe₃O₄/SiO₂/AuNPs) will have
82 great potential application in biotechnology.

83 Fowl typhoid (FT) and Pullorum disease (PD), were caused by *Salmonella*
84 *gallinarum* (*S. gallinarum*) and *Salmonella pullorum* (*S. pullorum*) respectively. FT, as an
85 acute or chronic septicemia infectious disease, primarily transmits by oral or respiratory
86 routes, and affects adult poultries or grower groups. PD is an acute systemic disease and
87 usually found in young birds.¹⁹ The disease can be transmitted by vertically and
88 horizontally to others with contaminated poultries that usually results in a high mortality
89 rate. A huge economic loss and serious threat for the development of intensive poultry
90 industry can be caused by *S. gallinarum* and *S. pullorum*. Therefore, establishing an
91 effective and fast detection measure for these two pathogens are required. Multilocus
92 enzyme electrophoresis and sequence analysis clearly stated that *S. pullorum* and *S.*
93 *gallinarum* both possess antigen O₁, O₉ and O₁₂, and exhibit high cross-reactivity with
94 each other, they are generally regarded as biotypes of the same serovar, resulting in that
95 they can be simultaneously detected.²⁰⁻²³ Barrow et al. deemed that it was difficult and
96 unnecessary to differentiate *S. pullorum* and *S. gallinarum* strictly.²⁴ And Oliveira et al.
97 used ELISA to assess serological response of chickens to *S. pullorum* and *S.*
98 *Gallinarum*.²⁵

99 The purpose of this study is to establish a sensitive and rapid amperometric

100 immunoassay method for food-borne pathogens detection. *S. gallinarum* and *S. pullorum*
101 was used as the analysis target models. MNPs were applied to increase the sensitivity of
102 our developed method, which takes advantages of magnetic particles as pre-concentrators.
103 In this study, The Fe₃O₄/SiO₂/AuNPs core-shell magnetic nanoparticles were synthesized
104 by anchoring AuNPs on Fe₃O₄ magnetic composites particles by strong bonding force
105 between –SH and AuNPs. AuNPs acted as the intermediary materials to link Fe₃O₄/
106 SiO₂–SH and antibody and get the immunomagnetic nanocomposites (Ab₁/AuMNP_s).
107 HRP labeled antibody against *S. pullorum* and *S. gallinarum* (HRP-Ab₂) was used as the
108 signal tag. *S. pullorum* and *S. gallinarum* bacteria in sample were captured by
109 Ab₁/AuMNP_s and separated from analyte samples by applying an external magnetic field.
110 The MNP–Salmonella complexes were re-dispersed in a buffer solution then exposed to
111 HRP-anti-*S. pullorum* and *S. gallinarum*. The final sandwich immunocomplexes were
112 then attached on the surface of the working electrodes of 4 channels screen printed
113 carbon electrode (4-SPCE) by an external magnetic field. Moreover, 4-SPCE was used to
114 shorten the detection time and improve the reproducibility. In addition, AuNPs were
115 electrodeposited on the working electrodes of 4-SPCE due to its signal amplification
116 function. CV was employed to determine *S. pullorum* and *S. gallinarum* via changes of
117 reduction peak current in the substrate solution of H₂O₂ and the electron mediator of
118 thionine included.

119

120 2. Experimental section

121 2.1. Reagents and solutions

122 *S. pullorum* and *S. gallinarum* (CMCC 50770) was employed as the target bacterium,
123 and *Escherichia coli* (*E. coli*, ATCC 8739), *Staphylococcus aureus* (*S. aureus*, ATCC
124 27217), *Enterobacter Sakazakii* (*E. sakazakii*, ATCC 29544), *Bacillus subtilis* (*B. subtilis*,
125 ACCC 11060), *Bacillus cereus* (*B. cereus*, ATCC 10987) and *Bacillus stearothermophilus*
126 (*B. stearothermophilus*, CICC 20137) were purchased from China Center
127 of Industrial Culture Collection (Beijing, China) and conserved in the laboratory of the
128 authors. Phosphate buffered saline (PBS, 0.01 M, pH 7.4) was used as control group.
129 Anti-*S. pullorum* and *S. gallinarum* were obtained from the China Institute of Veterinary
130 Drug Control (Beijing, China). HRP-labeled anti-*S. pullorum* and *S. gallinarum*

131 (HRP-Ab₂) were obtained from Shanghai Youke Biotechnology Co., Ltd. Chloroauric
132 acid was obtained from Hangzhou Chemical Reagent Co., Ltd. Thionine (Thi) was
133 obtained from Shanghai Zhongtai Chemical Reagent Co., Ltd. (Shanghai, China).
134 Tetraethyl orthosilicate (TEOS) was obtained from Aladdin Industrial Inc. (Shanghai,
135 China). 3-Mercaptopropyltriethoxysilane (MPTES) was obtained from Nanjing
136 Chengong Organic Silicone material Co., Ltd. (Nanjing, China). And other reagents were
137 all of analytical grade and the water used was doubly distilled.

138

139 **2.2. Apparatus**

140 CHI 1030 and CHI 760C electrochemical workstation were provided by Shanghai
141 ChenHua Instruments, Inc. (Shanghai, China). 4-Screen-printed carbon electrode
142 (4-SPCE) was developed by Rong Bin Biotechnology Co., Ltd. (Nanjing, China). The
143 diameter of disk-shaped working electrode was 0.25 cm, and the working electrode and
144 counter electrode were made of a carbon ink whereas the reference electrode was made of
145 Silver/Silver chloride (Ag/AgCl), they were all printed on a plastic support. The
146 nanostructures of electrode were characterized by SU-8010 field emission scanning
147 electron microscope (Tokyo, Japan). All electrochemical experiments were performed at
148 25 ± 2 °C.

149

150 **2.3. Synthesis of Fe₃O₄ magnetic nanoparticles**

151 The Fe₃O₄ nanoparticles were prepared according to the method of Ziyang Lu ²⁶.
152 1.35 mM FeSO₄·7H₂O was added to 70 mL double-distilled water, which had been
153 removed oxygen by continuously blowing with nitrogen for 30 min. Under vigorous
154 mechanical stirring and nitrogen protecting, 2.7 mM FeCl₃·6H₂O and 5 mL ammonia
155 solution were added to the above double-distilled water. After reacting 80 min at 80 °C,
156 Fe₃O₄ magnetic beads were isolated from the solution by a magnet and rinsed five times
157 by double-distilled water and diluted with water to a total volume of 60 mL.

158

159 **2.4. Synthesis of Fe₃O₄/SiO₂-SH nanoparticles**

160 The synthesis mechanism of Fe₃O₄/SiO₂-SH nanoparticles was displayed in Fig. 1A
161 and the details as follows: 60 mL ethanol solution and 9 mL ammonia solution were

162 mixed with 30 mL Fe₃O₄ magnetic beads solution in 100 mL flask. 1 mL TEOS was
163 dropped to the mixture slowly. With the help of stirring, the reaction was carried out for 2
164 h at 18 °C, then 0.5 mL MPTES was added, and reacted for 12 h. Fe₃O₄/SiO₂-SH
165 nanoparticles were isolated from the solution by a magnet and rinsed five times by
166 double-distilled water and diluted with water to a total volume of 6 mL.

167

168 **2.5. Synthesis of Fe₃O₄/SiO₂/AuNPs/Ab₁ nanocomposites**

169 Gold nanoparticles (AuNPs) were obtained according to the Frens method²⁷. In
170 brief, 1 mL of 1% HAuCl₄ and 100 mL ultra-pure water were mixed in a 250 mL flask. 5
171 mL of 1% sodium citrate solution was added quickly to the mixture after boiling, and the
172 boiling of the mixture was kept for another 15 min. As a result, the color of the solution
173 turned to wine red, implying the diameter of gold nanoparticles was between 5 nm and 20
174 nm. And colloidal gold solution was stored at 4 °C to prevent agglomerate.

175 Fe₃O₄/SiO₂/AuNPs nanocomposites (AuMNPs) were prepared by automatic
176 adsorption between AuNPs and Fe₃O₄/SiO₂-SH nanoparticles²⁸. Fig. 1B shows the
177 procedure of preparation. 20 μL Fe₃O₄/SiO₂-SH suspension (0.15 mg·mL⁻¹) dropped into
178 4 mL centrifuge tube with 1.5 mL colloidal gold solution, and incubated for 12-24 h at
179 room temperature. In order to make each Fe₃O₄/SiO₂-SH homogeneously combine with
180 AuNPs which can improve the stability of experiment results, the centrifuge tube was
181 shook slowly every four hours. AuMNPs were separated by a magnet, and rinsed three
182 times with PBS, then resuspended with 1 mL PBS.

183 Ab₁/AuMNPs was obtained as follows: 40 μL Anti-*S. pullorum* and *S. gallinarum*
184 (100 μg·mL⁻¹) and 1 mL AuMNPs suspension was mixed and stirred at 4 °C for 12 h.
185 Ab₁/AuMNPs was blocked by 1 mL 0.2% BSA at 4 °C for 1 h, then rinsed three times
186 with PBS, dispersed in 1 mL PBS, and stored at 4 °C for use.

187

188 **2.6. Preparation of electrochemical immunoassay method and measurements**

189 The AuNPs (25 nm) deposited 4-SPCE was prepared according to previous report²⁹.
190 The electrochemical reduction was performed with 4-SPCE by CV in a dispersion
191 containing 25 mg·L⁻¹ HAuCl₄ with a magnetic stirring and N₂ bubbling. The scan
192 potential was performed between -1.5 and 0.5 V at a scan rate of 25 mV·s⁻¹. Then the

193 electrode was rinsed with double-distilled water and dried with blowing N_2 at room
194 temperature (25 ± 2 °C).

195 The preparation of the immunoassay method and mechanism of rapid detection of *S.*
196 *pullorum* and *S. gallinarum* were displayed in Fig. 1C and D. The *S. pullorum* and *S.*
197 *gallinarum* was detected according to the following procedure: *S. pullorum* and *S.*
198 *gallinarum* was captured by 20 μL $\text{Ab}_1/\text{AuMNPs}$ in 1 mL sample solution, then separated
199 with a magnet and rinsed carefully three times. 20 μL HRP-Ab_2 ($7.8 \mu\text{g}\cdot\text{mL}^{-1}$) was
200 dropped into the above isolates and incubated for 30 min, rinsed carefully three times and
201 resuspended with 20 μL PBS. Then 5 μL $\text{HRP-Ab}_2/\text{Ag}/\text{Ab}_1/\text{AuMNPs}$ was dropped on the
202 $\text{AuNPs}/4\text{-SPCE}$ and adsorbed by magnet. 300 μL HAc-NaAc ($\text{pH}=6.5$, $0.1 \text{ mol}\cdot\text{L}^{-1}$)
203 containing $1.0 \text{ mmol}\cdot\text{L}^{-1}$ Thi and $0.7 \text{ mmol}\cdot\text{L}^{-1}$ H_2O_2 was dropped on the above modified
204 electrode. CV was conducted with a CHI 1030 at a scan rate of $25 \text{ mV}\cdot\text{s}^{-1}$ between -0.6 V
205 and -0.1 V . The detection of *S. pullorum* and *S. gallinarum* was performed by measuring
206 the reduction peak current change (ΔI_{pc}) of CV before and after the immune reaction.
207 Before the immunoreaction, the current response was recorded as I_1 . Due to the
208 accelerated decomposition of hydrogen peroxide by HRP, the current response of the
209 immunoassay method increased after the immunoreactions and was recorded as I_2 .
210 Therefore, changes of immunesensor current value (ΔI_{pc}) was expressed as $\Delta I_{\text{pc}} = I_2 - I_1$.
211 All experimental solutions were desecrated by nitrogen for at least 10 min before
212 measurement, and a nitrogen atmosphere was kept during the whole electrochemical
213 measurements. Three successive CV scans were performed for each measurement, the
214 last cycle was recorded.

215

216 **3. Results and discussion**

217 **3.1. Comparison of 4-SPCE and SPCE**

218 The reproducibility of 4-SPCE and SPCE were compared by using CV. As shown in
219 Fig. S.1, The RSD of 4-SPCE is 5.05% ($n=6$) and RSD of SPCE is 8.54%, indicating that
220 4-SPCE owns a better reproducibility than SPCE. The reason maybe that there are four
221 working electrodes on one 4-SPCE, meanwhile the four working electrodes of 4-SPCE
222 use the same auxiliary electrode and reference electrode, which avoid effects of the
223 external factors change. And it can simultaneously examine four samples under the same

224 test conditions. Conversely, different SPCEs can't be operated at the exact same condition
225 and don't have the completely consistent auxiliary electrode and reference electrode, that
226 is to say external factors can't be exactly the same. And for the high sensitivity of sensor
227 slight change will affect the reproducibility. Therefore, 4-SPCE is more stable and owns a
228 better reproducibility, it was chosen to use in this work.

229

230 3.2. Optimize the dosage of Fe₃O₄/SiO₂-SH

231 During the preparation of AuMNPs, two kinds of nanoparticles, Fe₃O₄/SiO₂-SH and
232 AuNPs, were linked by coupling agent to form a strong chemical bond. The composites
233 are stable by employing this method because the magnetic particles were coated with a
234 large amount of free thiol group (-SH) on the SiO₂ shell with
235 3-Mercaptopropyltriethoxysilane (MPTES) which has been found to exhibit a strong
236 binding force to AuNPs. In order to make each AuNMPs combine with sufficient anti-*S.*
237 *pullorum* and *S. gallinarum*, getting the best effect of enrichment for *S. pullorum* and *S.*
238 *gallinarum*. An experiment of different dosage of Fe₃O₄/SiO₂-SH from 0.075 to 0.375
239 mg·mL⁻¹ mixed with 1.5 mL AuNPs was carried out. Meanwhile Fe₃O₄/SiO₂ and PBS
240 were used as control groups (tube 1 and tube 2). As Fig. 2 shows that there is no
241 obviously difference between tube 1 (Fe₃O₄/SiO₂) and tube 2 (PBS), suggesting AuNPs
242 cannot react with Fe₃O₄/SiO₂. The solutions from tube 6 to 7 become transparent, and the
243 absorbance almost no longer changes, indicating all AuNPs have linked with
244 Fe₃O₄/SiO₂-SH. Therefore, 0.225 mg·mL⁻¹ Fe₃O₄/SiO₂-SH (tube 5) was selected as the
245 optimal condition.

246

247 3.3. Characterization of Ab₁/AuMNPs

248 Agglutination test was utilized to verify whether anti- *S. pullorum* and *S. Gallinarum*
249 had successfully linked with AuMNPs, 10 μL Ab₁/AuMNPs and 10 μL *S. pullorum* and *S.*
250 *Gallinarum* (10⁹ CFU·mL⁻¹) were dropped on glass slides, the results were recorded after
251 reacting for 1 min. Meanwhile *E. Coli* and PBS were used as control groups.
252 Ab₁/AuMNPs uniformly disperse in the solution of *E. Coli* and PBS as shown in Fig. 3B
253 and Fig. 3C, but agglomerate appears when *S. pullorum* and *S. Gallinarum* is added (Fig.
254 3A), indicating antibody has successfully linked with AuMNPs and Ab₁/AuMNPs have a

255 good dispersibility.

256

257 **3.4. Characterization of AuMNPs nanocomposite and AuNPs layer**

258 The morphology of bare 4-SPCE, AuNPs/4-SPCE and AuMNPs was characterized
259 using SEM. As shown in Fig. 4A, bare 4-SPCE is covered by smooth and uniform
260 nanoparticles with diameter of about 50 nm. Fig. 4B shows AuNPs with diameter of
261 about 25 nm are successfully electrodeposited on the working electrode. AuNPs were
262 introduced into the fabrication of the immunoassay method to enhance the
263 electrochemical signals and ensure the sensitivity of the test results. Fig. 4C shows
264 AuNPs successfully loaded on the surface of $\text{Fe}_3\text{O}_4/\text{SiO}_2\text{-SH}$, the size of which is about
265 250 nm. Fig. 4D displays the UV-Vis spectra of $\text{Fe}_3\text{O}_4/\text{SiO}_2\text{-SH}$, AuNPs and AuMNPs.
266 AuNPs show the absorption peak at about 520 nm (curve b). And there is no obvious
267 absorption peak from 400 to 700 nm (curve a). But an absorption peak appears at about
268 560 nm (curve c) after AuNPs immobilizing with $\text{Fe}_3\text{O}_4/\text{SiO}_2\text{-SH}$, suggesting that AuNPs
269 are successfully loaded on $\text{Fe}_3\text{O}_4/\text{SiO}_2\text{-SH}$.

270

271 **3.5. Electrochemical characteristics of the stepwise modified electrodes**

272 To investigate the effect of each component on the electrode, the redox behavior of a
273 reversible redox couple was recorded by CV after each modified step. Curves were
274 recorded in 1.0 mM Thi. Fig. 5 displays a pair of reversible redox peaks of Thi at the bare
275 4-SPCE (curve A). After electrodepositing in HAuCl_4 , the peak currents of the redox
276 peaks of 4-SPCE (curve B) significantly increases. But the redox current (curve C)
277 gradually decreases when $\text{Ab}_1/\text{AuMNPs}$ are dropped on the AuNPs/4-SPCE. Compared
278 with curve c, the redox current of $\text{Ag}/\text{Ab}_1/\text{AuMNPs}$ (curve D) significantly decreases.
279 This result indicates that *S. pullorum* and *S. gallinarum* is firmly captured to
280 $\text{Ab}_1/\text{AuMNPs}$ through the specific binding affinity between antigen and antibody. And
281 the formed electronic barriers hindered electron transfer toward the electrode surface,
282 result in the decreasing of peak current. After the addition of HRP-anti- *S. pullorum* and *S.*
283 *gallinarum*, the reduction peak current value (curve E) greatly increases, implying the
284 enzyme-labeled antibody is bound onto $\text{Ag}/\text{Ab}_1/\text{AuMNPs}$ through the immune interaction,
285 and the HRP catalyzes reduction of H_2O_2 with the assistance of an electron mediator,

286 which promotes electron transfer between the enzyme and the electrode. The
287 immunoassay method response is based on the following redox process:



291

292 **3.6. EIS characterization**

293 Electrochemical impedance spectroscopy (EIS) was employed to monitor the
294 interface properties of the carbon electrode surface during stepwise modifications^{30,31}.
295 Different stages of the modified electrode were characterized in the test base solution
296 containing 0.1 mM KCl and 5.0 mM $[\text{Fe}(\text{CN})_6]^{3-/4-}$. As seen from Fig. S.2, the R_{et} of
297 AuNPs/4-SPCE (curve B) significantly decreases compared with bare electrode (curve A),
298 due to the gold nanoparticles not only have a large specific surface area, but also own a
299 highly efficient electron transport property and electro-catalytic activity. The gold
300 nanoparticles greatly reduced the resistance and accelerated the rate of electron transfer.
301 When $\text{Ab}_1/\text{AuMNPs}$ was dropped onto the AuNPs/4-SPCE, a larger semicircle (curve C)
302 was observed, indicating the R_{et} greatly increased. After *S. pullorum* and *S. gallinarum*
303 was incubated with $\text{Ab}_1/\text{AuMNPs}$ and dropped onto the AuNPs/4-SPCE, the semicircle
304 (curve D) became larger, the antigen and $\text{Ab}_1/\text{AuMNPs}$ formed a barrier which impeded
305 electron transfer. Similar situations occurred when $\text{HRP-Ab}_2/\text{Ag}/\text{Ab}_1/\text{AuMNPs}$ was
306 dropped onto the AuNPs/4-SPCE (curve E). This result suggested that every step of the
307 modification were successful.

308

309 **3.7. Optimization of the experimental conditions**

310 To achieve the best performance, experimental conditions were optimized. The
311 results are given in Fig. S.3. the following experimental conditions were found to give
312 best results: (A) A concentration of H_2O_2 is $0.7 \text{ mmol} \cdot \text{L}^{-1}$; (B) A sample pH value of 6.5;
313 (C) Incubation time between anti-*S. pullorum* and *S. gallinarum* and *S. pullorum* and *S.*
314 *gallinarum* is 30 min; (D) Incubation temperature between anti-*S. pullorum* and *S.*
315 *gallinarum* and *S. pullorum* and *S. gallinarum* is $32 \text{ }^\circ\text{C}$; (E) Incubation time between *S.*
316 *pullorum* and *S. gallinarum* and $\text{HRP-anti-}S. pullorum$ and *S. gallinarum* is 30 min; (F)

317 Incubation temperature between *S. pullorum* and *S. gallinarum* and HRP-anti-*S. pullorum*
318 and *S. gallinarum* is 30 °C.

319

320 **3.8. Calibration curve of the immunoassay method**

321 Under these optimal conditions different concentrations of *S. pullorum* and *S.*
322 *gallinarum* (from 10^0 to 10^8 CFU·mL⁻¹) were detected. As Fig. 6A shows, with increasing
323 concentration of *S. pullorum* and *S. gallinarum*, the amount of HRP-labeled antibody
324 reacted with the immobilized *S. pullorum* and *S. gallinarum* increased, therefore, the ΔI_{pc}
325 increased. The plot of ΔI_{pc} versus the logarithm of *S. pullorum* and *S. gallinarum*
326 concentration shows a linear relationship in the concentration range from 10^2 to 10^6
327 CFU·mL⁻¹, and the linear regression equations is ΔI_{pc} (μA) = 0.3418x + 0.4698, R^2 =
328 0.9953. The limit of detection (*LOD*), which was defined as three times the standard
329 deviation of the blank sample measurements, was estimated to be 3.2×10^1 CFU·mL⁻¹
330 (Fig. 6A inset). As Table 1 shows, this sensor performance shows a potential in reducing
331 detection limit and more convenient as compared to other systems for bacteria detection.
332 In many of past reports, sample solution was dropped on the surface of SPCE to detect
333 pathogenic bacteria, and the volume of sample solution was always less than 30 μL ³²,
334 resulting in the detection limit can never be lower than 10^2 CFU·mL⁻¹. Because 30 μL 10^2
335 CFU·mL⁻¹ pathogen suspension only contains three bacteria in theory. And this problem
336 is well solved in this developed method.

337

338 **3.9. Specificity, reproducibility and stability of the immunoassay method**

339 The specificity and interference are very important for immunoassay method to
340 distinguish the target bacteria from other foodborne pathogens in samples. To prove the
341 specificity of the constructed immunoassay method, experiments were conducted using *E.*
342 *sakazakii*, *E. coli*, *B. subtilis*, *B. cereus*, *B. stearothermophilus* and *S. pullorum* and *S.*
343 *gallinarum*, and all of the bacteria solution concentrations were 10^6 CFU·mL⁻¹, PBS was
344 used as blank control. And *E. sakazakii* and *B. subtilis* were mixed with *S. pullorum* and *S.*
345 *gallinarum*, respectively. The results are displayed in Fig. 6B, the current increase
346 induced by *S. pullorum* and *S. gallinarum* ($\Delta I_{pc} = 2.3273 \pm 0.1393 \mu A$) is significantly
347 larger than the current increase induced by other bacteria and PBS, the largest

348 mean value and standard deviation was $0.7823 \pm 0.0241 \mu\text{A}$, suggesting the immunoassay
349 method had a high specificity for *S. pullorum* and *S. gallinarum*. And the ΔI_{pc} caused by
350 mixed bacteria solution contaminating *E. sakazakii* and *B. subtilis* just had inconspicuous
351 change, indicating the immunoassay method had a high anti-interference ability. The
352 specificity of immunoassay method was attributed to the highly specific antigen-antibody
353 immunoreactions.

354 A long-term storage stability of the prepared immunoassay method was also
355 measured. $\text{Ab}_1/\text{AuMNPs}$ were stored at 4°C when they were not in use, and
356 intermittently measured every five days with three modified electrodes, they retained
357 93.95% of their initial signal after a storage period of 30 days. Therefore, the modified
358 sensors towards *S. pullorum* and *S. gallinarum* owned good stability.

359 The reproducibility of the immunoassay method was investigated by independently
360 monitoring the reduction peak current values of five modified electrodes under same
361 experimental conditions. And the relative standard deviation (RSD) obtained at the
362 concentration of $10^6 \text{CFU}\cdot\text{mL}^{-1}$ was 5.33%. Therefore, the modified sensors towards *S.*
363 *pullorum* and *S. gallinarum* owned satisfying reproducibility. Different modified
364 electrodes for determination of *salmonella* were compared, and the dates are displayed in
365 Table 1. The performance of this sensor performance shows a potential in reducing
366 detection limit and more stable as compared to others for bacteria detection.

367

368 **3.10. Detection of *S. pullorum* and *S. gallinarum* in Real Samples**

369 In order to better verify the application of the newly developed immunoassay
370 method in practical sample detection, a series of food samples: chickens were bought
371 from market, the real sample were tested for *S. pullorum* and *S. gallinarum* by the China
372 national food safety standard (GB/T 17999.8-2008) for the detection of *S. pullorum* and *S.*
373 *gallinarum*. And we found that all of them were not affected by *S. pullorum* and *S.*
374 *gallinarum*. A blind method was used and performed by two teams. The detail steps were
375 as follows: one team randomly added a proper dose of *S. pullorum* and *S. gallinarum* into
376 the negative samples and mixed with other samples. Another team used the newly sensors
377 and the China national food safety standard (GB/T 17999.8-2008) in the assays. The two
378 teams were not allowed to interact during the whole process. The results were showed in

379 Table 2, the number in Table 2 is the number of true positive or negative results detected
380 by the corresponding methods. Accuracy is defined as the compliance between results got
381 by the developed method and the reference standard method for identical samples. By
382 comparing the results of electrochemical immunoassay method with standard culture
383 method, accuracy was 93.3%, the true positive rate was 94.2% and true negative rate was
384 87.5%. We find this sensor reveals a good agreement with standard method, indicating
385 that there was an acceptable accuracy and reliability of the immunoassay method. This
386 result revealed that the immunoassay method held great promise as a reliable tool for the
387 detection of *S. pullorum* and *S. gallinarumin* real samples.

388

389

390 4. Conclusions

391

392 A rapid and high-sensitive electrochemical immunoassay method based on
393 $\text{Fe}_3\text{O}_4/\text{SiO}_2/\text{AuNPs}$ and 4-SPCE has been successfully constructed for *S. pullorum* and *S.*
394 *gallinarumin* detection in this work. AuNPs were used as bridging materials between
395 biomolecules and $\text{Fe}_3\text{O}_4/\text{SiO}_2\text{-SH}$, AuNPs can easily immobilize the antibody onto the
396 $\text{Fe}_3\text{O}_4/\text{SiO}_2/\text{AuNPs}$ and retain high bioactivity of the adsorbed biomolecules.
397 Electrodeposited AuNPs on the working electrodes increased the current signal of this
398 method. This biosensor showed wide linear range, low detection limit and high specificity.
399 It can also be used for detection of *S. pullorum* and *S. gallinarumin* in real samples.
400 Importantly, this assay strategy remarkably improved the detect limit of immunoassay
401 method, provided a sensing platform for detection of *S. pullorum* and *S. gallinarumin*,
402 and the whole analytical process was shortened and simplified by using AuMNs and
403 4-SPCE. This immunoassay method can be used to develop other biosensors for
404 pathogenic bacteria and would become a useful tool for pathogenic microorganism
405 screening in clinical diagnostics, food safety and environmental monitoring.

406

407

408 Acknowledgments

409

410 This project was supported by the Food Science and Engineering the most important
411 discipline of Zhejiang province (JYTSP20141062). Zhejiang Public Innovation Platform
412 Analysis and testing projects (2015C37023). The Talent training provincial superior
413 paper funded project (1110JY1412001P). Postgraduate Scientific and Technological
414 Innovation Project of Zhejiang Gongshang University (3100XJ1514146) and Plans for
415 college students in Zhejiang Province science and technology innovation activities
416 (acrobatc tender grass talent programme) project (1110JQ4212048G). Project supported
417 by the fund of the National Natural Science Fund (30571623).

418

419

420

421

422 **Notes and references**

- 423 1. Afonso AS, Pérez-López B, Faria RC, et al. Electrochemical detection of Salmonella using gold
424 nanoparticles. *Biosensors and Bioelectronics* 2013; **40**(1): 121-6.
- 425 2. Salam F, Tothill IE. Detection of Salmonella typhimurium using an electrochemical immunosensor.
426 *Biosensors & Bioelectronics* 2009; **24**(8): 2630-6.
- 427 3. Gan N, Xiong P, Wang J, et al. A Novel Signal-Amplified Immunoassay for the Detection of
428 C-Reactive Protein Using HRP-Doped Magnetic Nanoparticles as Labels with the Electrochemical Quartz
429 Crystal Microbalance as a Detector. *Journal of analytical methods in chemistry* 2013; **2013**: 482316-.
- 430 4. Wu H, Zuo Y, Cui C, Yang W, Ma H, Wang X. Rapid Quantitative Detection of Brucella melitensis by
431 a Label-Free Impedance Immunosensor Based on a Gold Nanoparticle-Modified Screen-Printed Carbon
432 Electrode. *Sensors* 2013; **13**(7): 8551-63.
- 433 5. Huang J, Yang G, Meng W, Wu L, Zhu A, Jiao Xa. An electrochemical impedimetric immunosensor
434 for label-free detection of Campylobacter jejuni in diarrhea patients' stool based on
435 O-carboxymethylchitosan surface modified Fe₃O₄ nanoparticles. *Biosensors and Bioelectronics* 2010;
436 **25**(5): 1204-11.
- 437 6. Qi H, Li M, Zhang R, Dong M, Ling C. Double electrochemical covalent coupling method based on
438 click chemistry and diazonium chemistry for the fabrication of sensitive amperometric immunosensor.
439 *Analytica chimica acta* 2013; **792**: 28-34.
- 440 7. Wang Y, Li X, Cao W, et al. Facile fabrication of an ultrasensitive sandwich-type electrochemical
441 immunosensor for the quantitative detection of alpha fetoprotein using multifunctional mesoporous silica as
442 platform and label for signal amplification. *Talanta* 2014; **129**: 411-6.
- 443 8. Luo R, Zhang W, Cheng W, et al. A Novel Electrochemical Immunosensor for Detection of
444 AngiotensinII at a Glass Carbon Electrode Modified by Carbon Nanotubes/Chitosan Film. *Int J*
445 *Electrochem Sc* 2013; **8**(3): 3186-96.
- 446 9. Tang D, Yuan R, Chal Y. Ultrasensitive electrochemical immunosensor for clinical immunoassay
447 using thionine-doped magnetic gold nanospheres as labels and horseradish peroxidase as enhancer.
448 *Analytical chemistry* 2008; **80**(5): 1582-8.
- 449 10. Zhao X, Cai Y, Wang T, Shi Y, Jiang G. Preparation of Alkanethiolate-Functionalized Core/Shell
450 Fe₃O₄@Au Nanoparticles and Its Interaction with Several Typical Target Molecules. *Analytical chemistry*
451 2008; **80**(23): 9091-6.
- 452 11. Yang H-H, Zhang S-Q, Chen X-L, Zhuang Z-X, Xu J-G, Wang X-R. Magnetite-containing spherical
453 silica nanoparticles for biocatalysis and bioseparations. *Analytical chemistry* 2004; **76**(5): 1316-21.
- 454 12. Guo S, Dong S. Biomolecule-nanoparticle hybrids for electrochemical biosensors. *Trac-Trends in*
455 *Analytical Chemistry* 2009; **28**(1): 96-109.
- 456 13. Tang D, Su B, Tang J, Ren J, Chen G. Nanoparticle-Based Sandwich Electrochemical Immunoassay
457 for Carbohydrate Antigen 125 with Signal Enhancement Using Enzyme-Coated Nanometer-Sized
458 Enzyme-Doped Silica Beads. *Analytical Chemistry* 2010; **82**(4): 1527-34.
- 459 14. Liang R-P, Yao G-H, Fan L-X, Qiu J-D. Magnetic Fe₃O₄@Au composite-enhanced surface plasmon
460 resonance for ultrasensitive detection of magnetic nanoparticle-enriched α -fetoprotein. *Analytica Chimica*
461 *Acta* 2012; **737**(0): 22-8.
- 462 15. Deng Y, Qi D, Deng C, Zhang X, Zhao D. Superparamagnetic High-Magnetization Microspheres with
463 an Fe₃O₄@SiO₂ Core and Perpendicularly Aligned Mesoporous SiO₂ Shell for Removal of Microcystins.
464 *Journal of the American Chemical Society* 2008; **130**(1): 28-9.
- 465 16. Huang X, Tu H, Zhu D, Du D, Zhang A. A gold nanoparticle labeling strategy for the sensitive kinetic
466 assay of the carbamate-acetylcholinesterase interaction by surface plasmon resonance. *Talanta* 2009; **78**(3):
467 1036-42.
- 468 17. Lou S, Ye J-y, Li K-q, Wu A. A gold nanoparticle-based immunochromatographic assay: The
469 influence of nanoparticulate size. *Analyst* 2012; **137**(5): 1174-81.
- 470 18. Pollitt MJ, Buckton G, Piper R, Brocchini S. Measuring antibody coatings on gold nanoparticles by
471 optical spectroscopy. *Rsc Advances* 2015; **5**(31): 24521-7.
- 472 19. Barrow PA, Neto OCF. Pullorum disease and fowl typhoid—new thoughts on old diseases: a review.
473 *Avian Pathology* 2011; **40**(1): 1-13.

- 474 20. Baumler AJ, Tsois RM, Ficht TA, Adams LG. Evolution of host adaptation in *Salmonella enterica*.
475 *Infection and immunity* 1998; **66**(10).
- 476 21. Hu C, Dou W, Zhao G. Enzyme immunosensor based on gold nanoparticles electroposition and
477 Streptavidin-biotin system for detection of *S. pullorum* & *S. gallinarum*. *Electrochimica Acta* 2014; **117**:
478 239-45.
- 479 22. Baumler AJ, Hargis BM, Tsois RM. Tracing the origins of *Salmonella* outbreaks. *Science (New York,*
480 *NY)* 2000; **287**(5450).
- 481 23. Christensen JP, Olsen JE, Bisgaard M. Ribotypes of *Salmonella enterica* serovar *Gallinarum* biovars
482 *gallinarum* and *pullorum*. *Avian pathology : journal of the WVPA* 1993; **22**(4): 725-38.
- 483 24. Barrow PA, Berchieri A, Jr., Al-Haddad O. Serological Response of Chickens to Infection with
484 *Salmonella gallinarum*-*S. pullorum* Detected by Enzyme-Linked Immunosorbent Assay. *Avian Diseases*
485 1992; **36**(2): 227-36.
- 486 25. Oliveira GHdNnaA, Berchieri Júnior Â, Montassier HJ, Fernandes AC. Assessment of serological
487 response of chickens to *Salmonella Gallinarum* and *Salmonella Pullorum* by Elisa. *Revista Brasileira de*
488 *Ciência Avícola* 2004; **6**(2): 111-5.
- 489 26. Lu Z, Wang G, Zhuang J, Yang W. Effects of the concentration of tetramethylammonium hydroxide
490 peptizer on the synthesis of Fe₃O₄/SiO₂ core/shell nanoparticles. *Colloids and Surfaces A:*
491 *Physicochemical and Engineering Aspects* 2006; **278**(1-3): 140-3.
- 492 27. Kimling J, Maier M, Okenve B, Kotaidis V, Ballot H, Plech A. Turkevich method for gold
493 nanoparticle synthesis revisited. *The journal of physical chemistry B* 2006; **110**(32): 15700-7.
- 494 28. Gan N, Jin H, Li T, Zheng L. Fe₃O₄/Au magnetic nanoparticle amplification strategies for
495 ultrasensitive electrochemical immunoassay of alpha-fetoprotein. *Int J Nanomedicine* 2011; **6**: 3259-69.
- 496 29. Wang D, Dou W, Zhao G, Chen Y. Immunosensor based on electrodeposition of gold-nanoparticles
497 and ionic liquid composite for detection of *Salmonella pullorum*. *Journal of Microbiological Methods*
498 2014; **106**: 110-8.
- 499 30. Feng R, Zhang Y, Yu H, et al. Nanoporous PtCo-based ultrasensitive enzyme-free immunosensor for
500 zeranol detection. *Biosensors & bioelectronics* 2013; **42**: 367-72.
- 501 31. Li X, Guo Q, Cao W, Li Y, Du B, Wei Q. Enhanced electrochemiluminescence from luminol at
502 carboxyl graphene for detection of alpha-fetoprotein. *Analytical biochemistry* 2014; **457**: 59-64.
- 503 32. Labib M, Zamay AS, Kolovskaya OS, et al. Aptamer-based viability impedimetric sensor for bacteria.
504 *Analytical chemistry* 2012; **84**(21): 8966-9.
- 505 33. Huang J, Yang G, Meng W, Wu L, Zhu A, Jiao Xa. An electrochemical impedimetric immunosensor
506 for label-free detection of *Campylobacter jejuni* in diarrhea patients' stool based on
507 O-carboxymethylchitosan surface modified Fe₃O₄ nanoparticles. *Biosensors & bioelectronics* 2010; **25**(5):
508 1204-11.
- 509 34. Nguyen P-D, Tran TB, Nguyen DTX, Min J. Magnetic silica nanotube-assisted impedimetric
510 immunosensor for the separation and label-free detection of *Salmonella typhimurium*. *Sensors and*
511 *Actuators B: Chemical* 2014; **197**: 314-20.
- 512 35. Kuang H, Cui G, Chen XJ, et al. A One-Step Homogeneous Sandwich Immunosensor for *Salmonella*
513 Detection Based on Magnetic Nanoparticles (MNPs) and Quantum Dots (QDs). *Int J Mol Sci* 2013; **14**(4):
514 8603-10.
- 515 36. Dong J, Zhao H, Xu M, Ma Q, Ai S. A label-free electrochemical impedance immunosensor based on
516 AuNPs/PAMAM-MWCNT-Chi nanocomposite modified glassy carbon electrode for detection of
517 *Salmonella typhimurium* in milk. *Food Chem* 2013; **141**(3): 1980-6.

518

519

520

521

522

523 **Caption**

524 Fig. 1. Schematic diagram of the modification process of electrochemical immunoassay
525 method and measure mechanism: (A) The synthesis process of $\text{Fe}_3\text{O}_4/\text{SiO}_2\text{-SH}$
526 nanoparticles; (B) The synthesis process of $\text{Ab}_1/\text{AuMNPs}$; (C) The process of *S. pullorum*
527 and *S. gallinarum* being captured from samples by $\text{Ab}_1/\text{AuMNPs}$ and the formation of
528 $\text{HRP-Ab}_2/\text{Ag}/\text{Ab}_1/\text{AuMNPs}$; (D) $\text{HRP-Ab}_2/\text{Ag}/\text{Ab}_1/\text{AuMNPs}$ dropped on the
529 $\text{AuNPs}/4\text{-SPCE}$, the principle of electrochemical detection.

530 Fig. 2. Optimization of the $\text{Fe}_3\text{O}_4/\text{SiO}_2\text{-SH}$ dosage: (1) $0.150 \text{ mg}\cdot\text{mL}^{-1} \text{Fe}_3\text{O}_4/\text{SiO}_2$; (2)
531 PBS ; (3) $0.075 \text{ mg}\cdot\text{mL}^{-1} \text{Fe}_3\text{O}_4/\text{SiO}_2\text{-SH}$; (4) $0.150 \text{ mg}\cdot\text{mL}^{-1} \text{Fe}_3\text{O}_4/\text{SiO}_2\text{-SH}$; (5) 0.225
532 $\text{mg}\cdot\text{mL}^{-1} \text{Fe}_3\text{O}_4/\text{SiO}_2\text{-SH}$; (6) $0.300 \text{ mg}\cdot\text{mL}^{-1} \text{Fe}_3\text{O}_4/\text{SiO}_2\text{-SH}$; (7) $0.375 \text{ mg}\cdot\text{mL}^{-1}$
533 $\text{Fe}_3\text{O}_4/\text{SiO}_2\text{-SH}$ was dropped into 1.5 mL colloidal gold solution.

534 Fig. 3. The agglutination test results of (A) 10 μL *S. pullorum* and *S. Gallinarum*, (B) 10
535 μL *E. Coli*, (C) 10 μL PBS was respectively mixed with 10 μL IMB .

536 Fig. 4. FE-SEM images of (A) bare SPCE; (B) AuNPs/SPCE ; (C) TEM images of
537 AuMNPs ; (D) UV-vis absorption spectrum of $\text{Fe}_3\text{O}_4/\text{SiO}_2$ (a), AuNPs (b) and AuMNPs
538 (c).

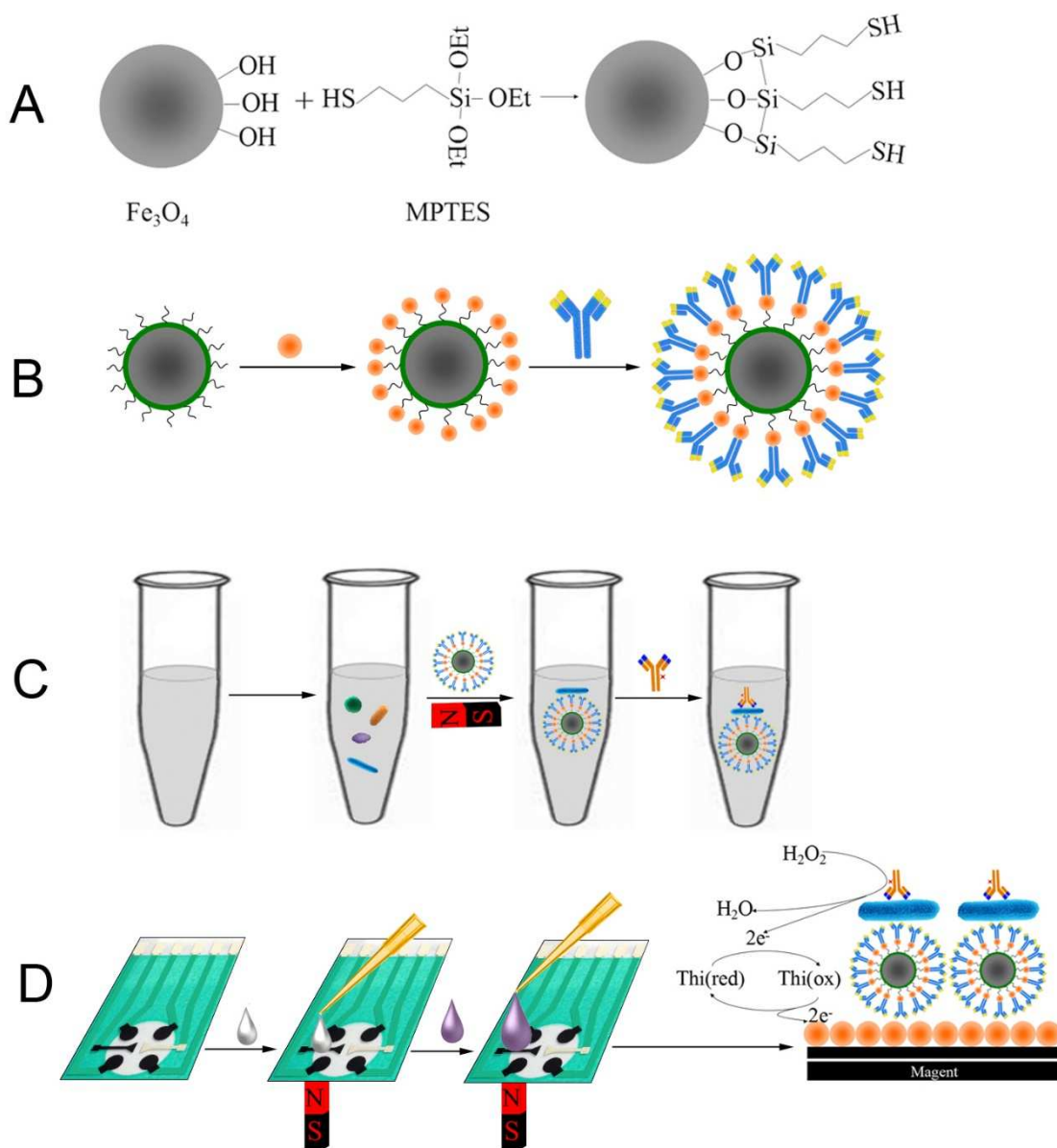
539 Fig. 5. Current curve of different modified electrode (A) Bare 4-SPCE, (B)
540 $\text{AuNPs}/4\text{-SPCE}$, (C) Anti-*S. pullorum* and *S. gallinarum}/\text{AuMNPs}/4\text{-SPCE}, (D) *S.*
541 *pullorum* and *S. gallinarum}/\text{Anti-}S. pullorum* and *S. gallinarum}/\text{AuMNPs}/4\text{-SPCE}, (E)
542 $\text{HRP-anti-}S. pullorum$ and *S. gallinarum}/S. pullorum* and *S. gallinarum}/\text{Anti-}S. pullorum*
543 and *S. gallinarum}/\text{AuMNPs}/4\text{-SPCE}***

544 Fig. 6. The performances of immunoassay method: (A) The ΔIpc of different
545 concentrations of the logarithm *S. pullorum* and *S. gallinarum*(Inset: Linear relation
546 between the reduction peak current change (ΔIpc) and of *S. pullorum* and *S. gallinarum*
547 concentration.); The specificity of immunoassay method for *S. pullorum* and *S.*
548 *gallinarum*: (B) The modified electrodes incubated with *S. pullorum* and *S. gallinarum*,
549 *E.sakazakii*, *B. cereus*, *B. subtilis*, *E. coli*, and *B. stearothermophilus*, PBS (0.01 M, pH
550 7.4) under the best reaction conditions, and mixed bacteria liquid A and B (*S. pullorum*
551 and *S. gallinarum* mixed with *E.sakazakii* and *B. subtilis*), respectively.

552 Table 1 Comparison of recently reported methods for determination of *salmonella*.

553 Table 2 Accuracy experimental results of a group modified electrodes (n=60).

554



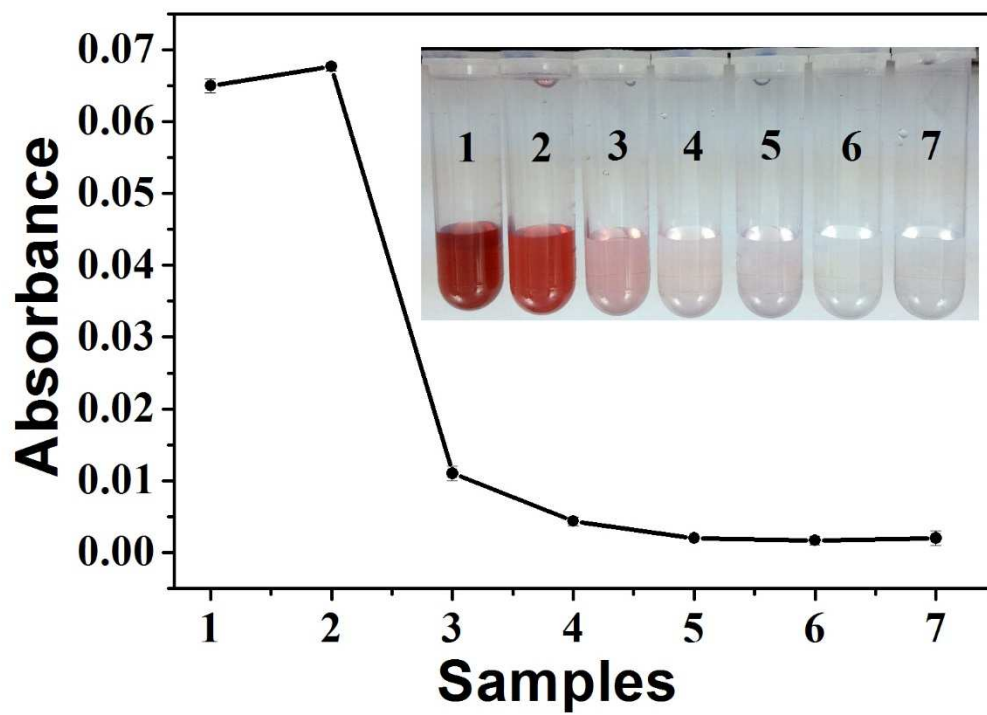
555

556 \bullet : Fe_3O_4 ; \sim : MPTES; \bullet : AuNPs; Y : anti- *S. pullorum* and *S. gallinarum*; \bullet ,
 557 \bullet , \bullet : other Bacteria; Y : *S. pullorum* and *S. gallinarum*; **Magnet**: Magnet; \bullet :
 558 Ag/Ab₁/AuMNPs; \bullet : Thionine solution.

559

560 Fig. 1

561



562

563 Fig. 2

564

565

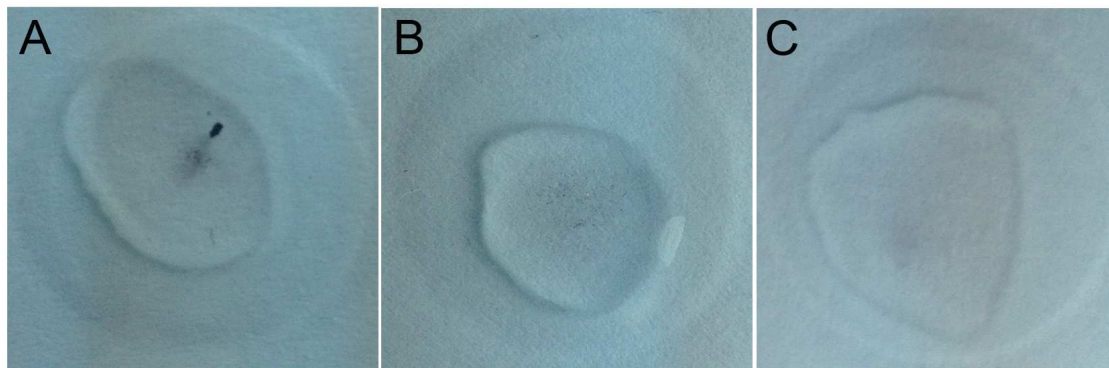
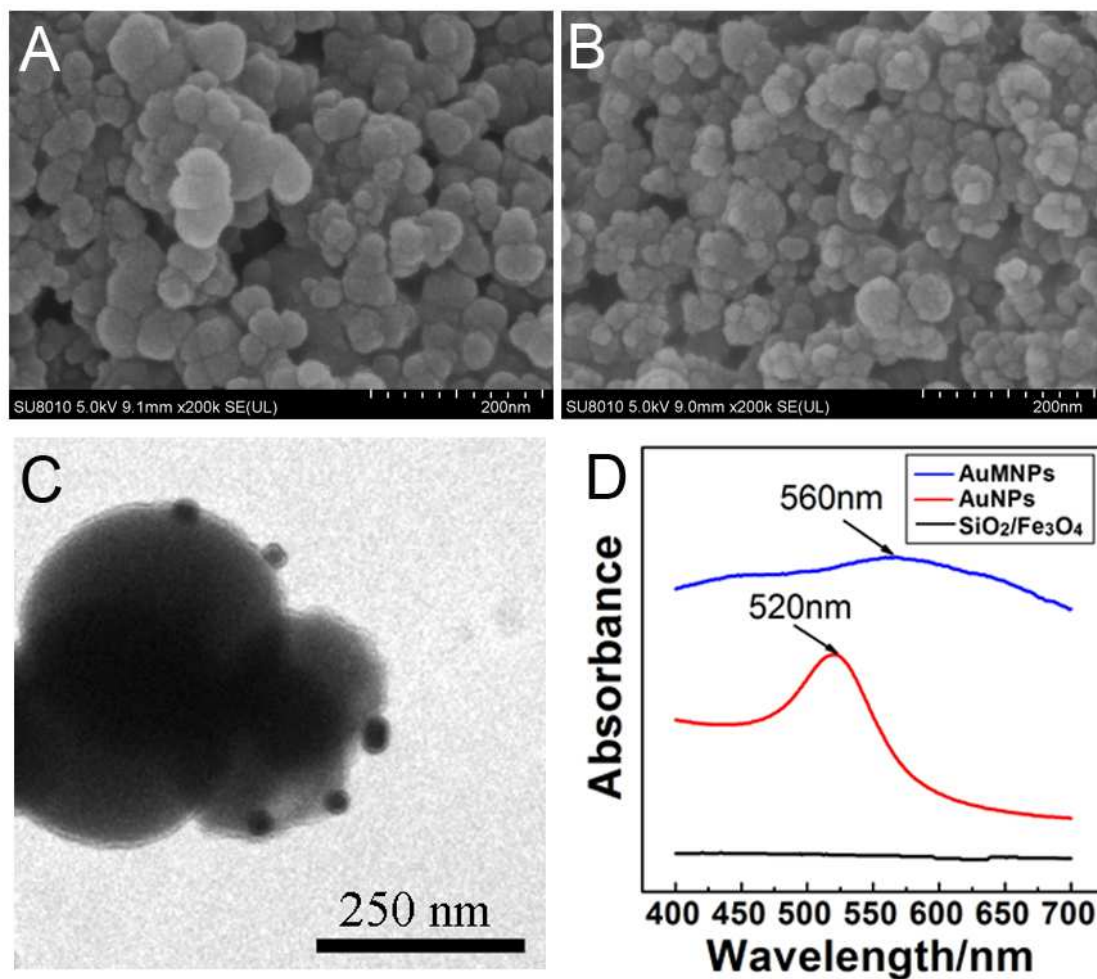
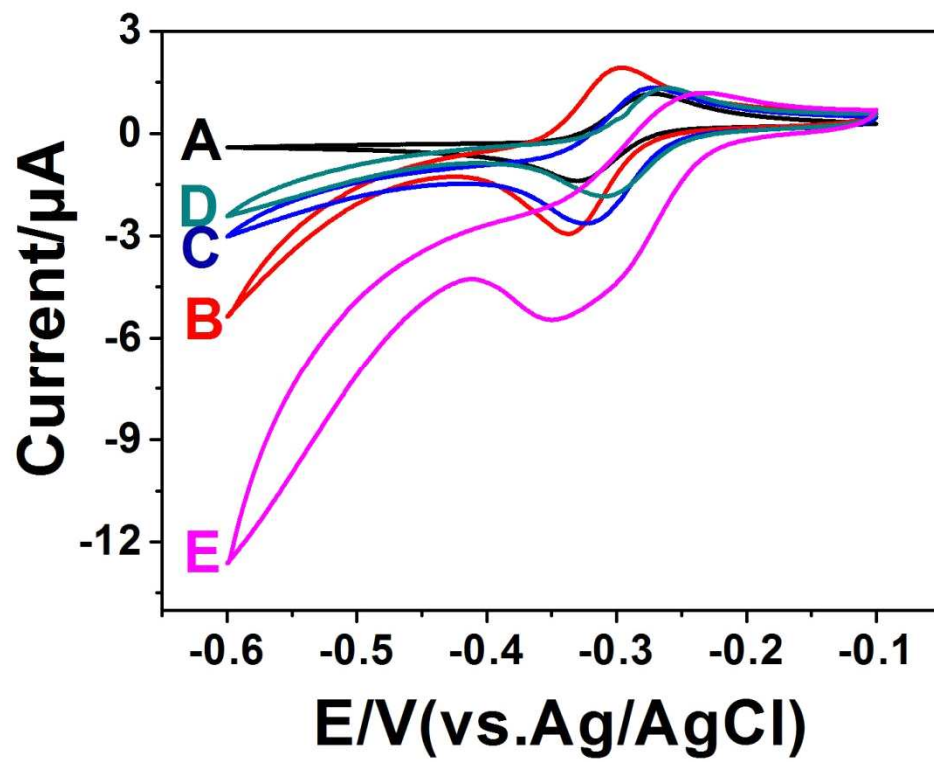
566
567
568
569

Fig. 3

570
571572
573 Fig. 4
574

575



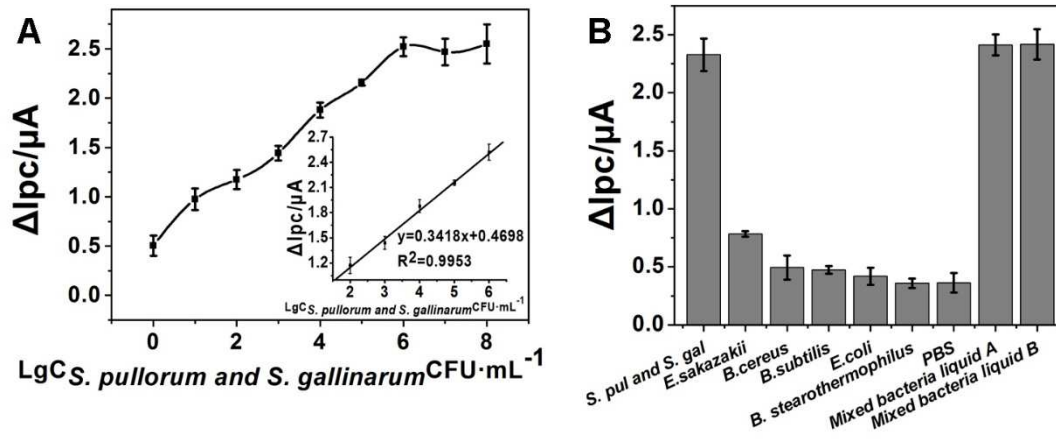
576

577 Fig. 5

578

579

580



581

582 Fig. 6

583

584

585

Material/method used	Analytical ranges (CFU·mL ⁻¹)	LODs (CFU·mL ⁻¹)	Reproducibility	Interferences
OCMCS/Fe ₃ O ₄ /GCE (EIS)	10 ³ – 10 ⁷	1.0 × 10 ³	6.3%	33
MBs-pSAb/S/sSAb-AuNPs/S PCE(DPV)	10 ³ – 10 ⁶	1.43 × 10 ²	2.4%	1
MSNTs/IDAM(EIS)	10 ³ – 10 ⁷	10 ³	—	34
MNPs/QDs(—)	2.5 × 10 ³ – 1.95 × 10 ⁸	5.0 × 10 ²	—	35
AuNPs/PAMAM/MWCNT/Chi/GCE (EIS)	10 ³ –10 ⁶	5.0 × 10 ²	3.8%	36
Fe ₃ O ₄ /SiO ₂ /AuNPs/AuNPs/4-SPCE(CV)	10 ² – 10 ⁶	3.2 × 10 ¹	5.3%	This work

586

587 *AuNPs* gold nanoparticles, *PAMAM* Poly(amidoamine), *MWCNT* Multi wall carbon
588 nanotubes, *Chi* Chitosan, *GCE* glassy carbon electrodes, *OCMCS*
589 O-Carboxymethylchitosan surface, *MBs-pSAb* magnetic beads modified with primary
590 antibodies, *S Salmonella*, *sSAb-AuNPs* AuNPs modified with secondary antibodies,
591 *MSNTs* magnetic silica nanotubes, *IDAM* interdigitated array microelectrodes, *MNPs*
592 magnetic nanoparticles, *QDs* quantum dots.

593 Table 1

594

595

		Immunoassay method		
		Positive	Negative	Total
GB	Positive	49	3	52
	Negative	1	7	8
	Total	50	10	60

596 Table 2